Waves Random Media **11** (2001) 149–162 www.iop.org/Journals/wr PII: S0959-7174(01)20537-0

Solitons in random media with long-range correlation

J Garnier

Centre de Mathématiques Appliquées, Centre National de la Recherche Scientifique, Unité Mixte de Recherche 7641, Ecole Polytechnique, 91128 Palaiseau Cedex, France

E-mail: Josselin.Garnier@polytechnique.fr

Received 8 January 2001, in final form 6 March 2001

Abstract

A statistical approach of the propagation of solitons in media with a spatially random potential is developed. Applying the inverse scattering transform several regimes are demonstrated which are determined by the mass and the velocity of the incoming soliton as well as by the correlation length of the random potential. Namely, the mass of the soliton is conserved if its initial amplitude is large enough. If the initial mass is small, then the mass decays with the length of the system. The decay rate is exponential in the case of a white noise perturbation, but it obeys a power law if the carrier wavenumber of the soliton lies in the tail of the spectrum of the potential. Furthermore, the scattered radiation propagates in a backward direction in the case of a white noise perturbation, while it propagates in a forward direction (with the same carrier wavenumber as the soliton) in the case of a coloured noise with long-range correlation.

1. Introduction

Over the last decade many papers have been devoted to the study of propagation of solitons through random media. Most of them have been concerned with a perturbation of the potential [1–4]. Numerical modelling of the nonlinear Schrödinger (NLS) equation with a random linear potential confirms this theory [5,6]. There also exist experimental investigations of the propagation of nonlinear waves in random media [7, 8], describing the Korteweg–de Vries- (KdV-) type wave propagation, that may have qualitative relevance to the analytical work where the NLS case is addressed since both NLS and KdV equations are completely integrable systems.

We shall consider the one-dimensional nonlinear Schrödinger equation with a random potential. As a first motivation we look at the continuum limit of a nonlinear Anderson model [1], but the same model can also be derived from the continuum limit corresponding to randomly dispersed impurities [9]. This problem actually arises in this form in a number of problems in nonlinear optics [10] as well as in solid state physics [11–13]; as an example, it can be derived in the small-amplitude limit for the sine-Gordon and ϕ^4-models [14]. Our contribution consists in the study of the long-scale behaviour of this system in the asymptotic

0959-7174/01/030149+14$30.00

framework where the amplitude of the random potential tends to small values and the size of the system tends to large values.

The problem has been studied and the influence of the nonlinearity is now well understood. These results have been derived for a white noise, or a white-noise-type model. We refer, in particular, to the survey paper by Gredeskul and Kivshar [15]. In [16] we revisited these results from a mathematical point of view, and we proved that the results actually hold true for a large class of coloured noises. The basic tool of our approach relies on a perturbed inverse scattering transform [17]. The general form of the effective system that governs the soliton dynamics was established in a general framework and discussed in configurations close to the white noise case. Recently, we discovered that the discussion proposed in [16] is incomplete in that the influence of long-range correlation in the noise may induce drastic changes in the soliton dynamics. This paper is devoted to a thorough study of this problem. More exactly, we shall deal with the propagation of a soliton whose carrier wavenumber lies in the tail of the noise spectrum. The interplay of the correlation length of the medium and the characteristic lengths of the soliton (related to its width and velocity) will be shown to play an important role.

Our main aim is to demonstrate that original and unexpected behaviours can be exhibited in the sense that they are not encountered when studying white noise perturbations. We shall show that a coloured noise is less critical in terms of backscattering or localization effects, but it may induce the conversion of the original soliton (of nonlinear nature) into dispersive radiation (of linear nature) that propagates with the same velocity as the soliton.

We consider a perturbed NLS equation with a random potential:

$$\mathrm{i}u_t + u_{xx} + 2|u|^2 u = \varepsilon m(x) u. \tag{1}$$

The small parameter $\varepsilon > 0$ characterizes the amplitude of the potential. m is assumed to be a zero-mean, stationary and ergodic process. The Fourier transform of the autocorrelation function of the process m is

$$d(k) = 2\int_0^\infty \mathbb{E}[m(0)m(x)]\cos(kx)\,\mathrm{d}x \tag{2}$$

which is non-negative since it is proportional to the k-frequency evaluation of the power spectral density of the stationary process m (Wiener–Khintchine theorem [18]). Throughout the paper the bandwidth of the power spectral density will play an important role so we denote by $1/l_c$ its typical width.

When there is no random potential in the underlying medium the partial differential equation (1) is completely integrable and admits soliton solutions:

$$u_0(t,x) = \frac{N_0}{2}\frac{\exp\mathrm{i}\left(\frac{1}{2}V_0(x-V_0t) + \frac{1}{4}(N_0^2+V_0^2)t\right)}{\cosh\left(\frac{1}{2}N_0(x-V_0t)\right)}. \tag{3}$$

The mass $\int |u_0|^2\,\mathrm{d}x$ and the velocity of the soliton are, respectively, N_0 and V_0.

If we restrict ourselves to the linear problem (by neglecting the cubic term on the right-hand side of equation (1)), then the problem of the propagation of a monochromatic wave in a random medium reduces to the second-order ordinary differential equation with a random coefficient (the Helmholtz equation with a spatially random refractive index):

$$-u_{xx} + \varepsilon m(x) u = k^2 u \tag{4}$$

where k is the wavenumber. This leads to the well known phenomenon of strong localization, which means that the transmission coefficient $T^\varepsilon(L,k)$ of a slab of random medium decays exponentially with the size of the slab L [9, 19]:

$$\frac{1}{L}\ln T^\varepsilon(L,k) \stackrel{L\to\infty}{\longrightarrow} -\frac{1}{L_{loc}^\varepsilon(k)}. \tag{5}$$

Furthermore, the so-called localization length $L^{\varepsilon}_{loc}(k)$ can be expanded in powers of the amplitude of the potential ε [20]:

$$\frac{1}{L^{\varepsilon}_{loc}(k)} = \frac{d(2k)}{4k^2}\varepsilon^2 + \mathrm{O}(\varepsilon^3). \tag{6}$$

If k lies in the tail of the spectrum of the random potential, then $d(2k)$ is very small. In this framework, the localization length of a monochromatic wave is very large. This means that a high-frequency wave is hardly sensitive to the random potential so that it can propagate over very large distances.

2. Soliton dynamics

We use the inverse scattering transform to study our problem. Indeed, the random potential induces variations of the spectral data [21]. Calculating these changes we are able to find the asymptotic evolution of the field and calculate the characteristic parameters of the wave. We are interested in the asymptotic dynamics of the soliton propagating over the long distance L/ε^2. The total mass and energy are conserved but the discrete and continuous components evolve during the propagation. The evolution of the continuous component corresponding to the radiation is found from the evolution equations of the Jost coefficients. The evolutions of the soliton parameters are then derived from the conservation of the total mass and energy. The main results stated in [16] and sketched out in the appendix are the following. First, the event 'the transmitted wave consists of one soliton plus some radiation' occurs with very high probability for small ε, and second, the soliton dynamics is governed by non-random equations in the asymptotic framework $\varepsilon \to 0$, where only the power spectral density of the random potential appear:

$$\frac{\mathrm{d}N}{\mathrm{d}L} = -\int_{-\infty}^{\infty} n(\lambda, N, V)\,\mathrm{d}\lambda \tag{7a}$$

$$\frac{\mathrm{d}V}{\mathrm{d}L} = -\frac{1}{2}\int_{-\infty}^{\infty}\left(\frac{16\lambda^2}{NV} + \frac{N}{V} - \frac{V}{N}\right) n(\lambda, N, V)\,\mathrm{d}\lambda \tag{7b}$$

where $n(\lambda, N, V)$ is the scattered mass density per unit length for the coloured noise model with power spectral density $d(k)$:

$$n(\lambda, N, V) = C(\lambda, N, V)d(\kappa(\lambda, N, V)) \tag{8}$$

$C(\lambda, N, V)$ is the scattered mass density per unit length for the normalized white noise model ($d(k) \equiv 1$):

$$C(\lambda, N, V) = \frac{\pi}{2^4 V^6}\frac{\left((4\lambda - V)^2 + N^2\right)^2}{\cosh^2\left(\pi\frac{V^2-N^2-16\lambda^2}{4NV}\right)} \tag{9}$$

and $\kappa(\lambda, N, V)$ is equal to

$$\kappa(\lambda, N, V) = \frac{(4\lambda - V)^2 + N^2}{4V}. \tag{10}$$

3. The small-mass regime $N_0 \ll V_0$

When $N \ll V$ the scattered mass density for the white noise model presents a main peak around $-V/4$:

$$C\left(\lambda = -\frac{V}{4} + Nx, N, V\right) = \frac{\pi}{V^2\cosh^2(2\pi x)} \tag{11}$$

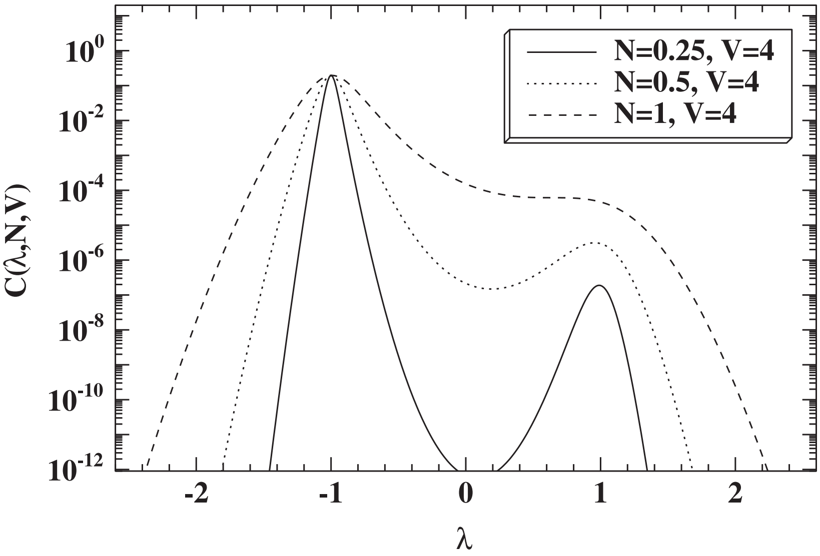

Figure 1. Mass density scattered by a soliton with weak amplitude in the white noise model ($d(k) \equiv d(0) = 1$). One can see the main peak around $\lambda = -V/4$, and the secondary peak around $\lambda = V/4$.

and also a secondary peak around $V/4$, which is much weaker than the first one (see figure 1) because of the factor N^4/V^4:

$$C\left(\lambda = \frac{V}{4} + Nx, N, V\right) = \frac{N^4}{V^4} \frac{\pi(1+16x^2)^2}{16V^2\cosh^2(2\pi x)}. \tag{12}$$

Accordingly, in the white noise model, the dynamics is imposed by the main peak, so that system (7) can be solved analytically yielding $V(L) = V_0$ and the exponential decay of the mass. In the coloured noise model we take into account the influence of the power spectral density of the noise. The system (7) can then be simplified. We find that the velocity is preserved, while the mass decays to 0 according to the differential equation

$$\frac{\mathrm{d}N}{\mathrm{d}L} = -\frac{d(V_0)}{V_0^2}N - \frac{\bar{d}(N^2/(4V_0))}{V_0^6}N^5 \tag{13a}$$

$$\bar{d}(\bar{N}) = \int_{-\infty}^{\infty} d\left(\bar{N}(1+16x^2)\right) \frac{\pi(1+16x^2)^2}{16\cosh^2(2\pi x)}\,\mathrm{d}x. \tag{13b}$$

Note that we cannot get rid of the term that originates from the secondary peak unlike the white noise model because $\bar{d}(N^2/(4V_0))$ may be much larger than $d(V_0)$. It appears here the two important characteristic lengths of the soliton:

$$l_0 := \frac{4V_0}{N_0^2} \qquad l_1 := \frac{1}{V_0}. \tag{14}$$

Note that the l_0 is much larger than l_1 in the small-mass regime. Although the width $1/N_0$ of the soliton envelope seems a natural characteristic length, we shall see in this paper that the relevant characteristic lengths which play a role in the random scattering are l_0 and l_1. More exactly we can distinguish three regimes depending on the ratios between the correlation length l_c and the characteristic lengths l_0 and l_1.

3.1. Short-range correlation

Here we assume that the correlation length is of the same order as or smaller than the characteristic length l_1: $l_c \sim l_1$ or $l_c \ll l_1$. On the one hand this implies $l_0 \gg l_c$, so that for any $N \leqslant N_0$ we have $\bar{d}(N^2/(4V_0)) \simeq 2d(0)/15$. On the other hand, $l_c \leqslant l_1$ implies that $d(V_0)$ is of the same order as $d(0)$, so that the second term on the right-hand side of (13a) is very negligible compared with the first one. Accordingly, the mass N decreases exponentially with L:

$$N(L) = N_0 \exp\left(-\frac{L}{L_{loc}}\right) \qquad L_{loc} = \frac{V_0^2}{d(V_0)}. \tag{15}$$

We obtain exactly the same result as in the white noise model. This indicates that the white noise model is valid as soon as $l_c \leqslant l_1$ or even $l_c \sim l_1$. We can give a simple physical explanation of this exponential regime. In the limit case $N_0/V_0 \to 0$, the incoming soliton can be approximated by a linear wavepacket:

$$u_0(t,x) \simeq \int_{-\infty}^{+\infty} \mathrm{d}k\, \hat{\phi}_0(k)\, \mathrm{e}^{\mathrm{i}kx - \mathrm{i}k^2 t} \tag{16a}$$

$$\hat{\phi}_0(k) = \tfrac{1}{2}\cosh^{-1}\left(\frac{\pi}{N_0}(k-k_0)\right) \tag{16b}$$

whose spectrum $\hat{\phi}_0$ is peaked at the wavenumber $k_0 := V_0/2$. Equation (15) is therefore in agreement with the linear approximation, where the random potential gives rise to the exponential decay of the transmittivity of a linear wavepacket. Note also that the radiation is scattered backward since the spectrum of the radiation is concentrated at $\lambda = -V_0/4$ which corresponds to the wavenumber $k = -V_0/2$.

3.2. Medium-range correlation

Here we analyse the configuration $l_1 \ll l_c \ll l_0$. The inequality $l_0 \gg l_c$ implies that, for any $N \leqslant N_0$, we have $\bar{d}(N^2/(4V_0)) \simeq 2d(0)/15$. Then the velocity is constant while the decay of the mass is governed by

$$\frac{\mathrm{d}N}{\mathrm{d}L} = -\frac{d(V_0)}{V_0^2}N - \frac{2d(0)}{15V_0^6}N^5. \tag{17}$$

If the ratio $l_1 \ll l_c$ is small enough so that $2d(0)N_0^4/(15V_0^4) \ll d(V_0)$, then the main peak of the scattered mass density is so reduced that the second term actually prevails over the first one on the right-hand side of equation (13a). Accordingly, the decay rate of the mass of the soliton N obeys a power law:

$$N(L) = N_0\left(1 + \frac{L}{L_{dec}}\right)^{-1/4} \qquad L_{dec} = \frac{15V_0^6}{8d(0)N_0^4}. \tag{18}$$

Furthermore, radiation is emitted in the forward direction, and its spectrum is centred around the carrier wavenumber of the soliton $V_0/2$. So, in this regime, there is neither backscattering nor localization. However, the soliton is progressively converted into dispersive radiation that propagates in the forward direction.

This holds true rigorously if the power spectral density vanishes around V_0. If not, since N is decaying, the ratio $2d(0)N(L)^4/(15V_0^4)$ also decays, so that when N becomes small enough, this ratio becomes smaller than $d(V_0)$ and decreasing the mass again obeys the exponential law (15). The crossover between the power decay and the exponential decay occurs when L reaches the value $L_{cros,1}$,

$$L_{cros,1} = \left(\frac{2d(0)N_0^4}{15d(V_0)V_0^4} - 1 \right) L_{dec}. \tag{19}$$

3.3. Long-range correlation

Here we analyse the configuration $l_0 \ll l_c$. Then the velocity is constant while the decay of the mass depends on the tail of the spectrum of the random potential.

3.3.1. Power decay of the power spectral density. To discuss this dependence we shall first consider that the power spectral density has a power-law decay: $d(k) = \sigma^2 l_c^{1-p} k^{-p}$, for $|k| l_c \gg 1$. Note that a finite variance $\mathbb{E}[m(0)^2] < \infty$ implies $p > 1$. Denoting

$$c_p = \frac{\pi}{16} \int_{-\infty}^{\infty} \frac{\mathrm{d}x}{(1+16x^2)^{p-2}\cosh^2(2\pi x)} \tag{20}$$

we can rewrite the system (13) as

$$\frac{\mathrm{d}N}{\mathrm{d}L} = -\sigma^2 l_c^{1-p} \frac{N}{V_0^4} \left(\left(\frac{1}{V_0} \right)^{p-2} + 4c_p \left(\frac{4V_0}{N^2} \right)^{p-2} \right). \tag{21}$$

Since $l_0 \gg l_1$ we should distinguish the cases $p < 2$, $p = 2$ and $p > 2$.

If $p < 2$, then the first term within the big parentheses of the right-hand side of equation (21), which originates from the main peak of the scattered mass density, is dominant, so that we obtain the usual exponential decay.

If $p > 2$, then the second term prevails over the first one, so that the decay rate of the mass of the soliton N is rapid and apparently leads to the disintegration of the soliton at distance L_{dis}:

$$N(L) = N_0 \left(1 - \frac{L}{L_{dis}} \right)^{1/(2p-4)} \tag{22a}$$

$$L_{dis} = \frac{32}{(p-2)c_p \sigma^2 l_c} \frac{V_0^6}{N_0^4} \left(\frac{l_c}{l_0} \right)^p. \tag{22b}$$

As in the case of medium-range correlation, radiation is emitted in the forward direction, and its spectrum is centred around the carrier wavenumber of the soliton. This means that the soliton is progressively converted into forward-going dispersive radiation. However, the complete disintegration does not occur, because just before it should occur, at distance $L_{cros,2}$:

$$L_{cros,2} = \left(1 - \left(\frac{l_c}{l_0} \right)^{p-2} \right) L_{dis} \tag{23}$$

the quantity $4V_0/N^2(L)$ becomes larger than l_c. Then we get back the regime described in section 3.2 that is characterized by a decay of the mass as $L^{-1/4}$.

3.3.2. Complements on the critical power decay. Let us consider in more detail the case when the decay of the power spectral density is k^{-2}:

$$d(k) \simeq \sigma^2 l_c^{-1} k^{-2} \qquad |k| l_c \gg 1. \tag{24}$$

This configuration is of particular interest since a decay as k^{-2} for the power spectral density is very normal. For instance, the two following classical models belong to this class. Both of them are stepwise constant processes that are constant over elementary intervals $[x_j, x_{j+1})$ and take values v_j over the jth interval. The v_js are assumed to be independent random variables with zero mean and variance σ^2. First assume that the x_j are deterministic and that all intervals have the same length l_c: $x_j = jl_c$. Then the autocorrelation function is

$$\mathbb{E}[m(0)m(x)] = \sigma^2 \mathbf{1}_{|x|\leqslant l_c}\left(1 - \frac{|x|}{l_c}\right) \tag{25}$$

so that the power spectral density is

$$d(k) = \sigma^2 l_c \mathrm{sinc}\left(\frac{kl_c}{2}\right)^2$$

where $\mathrm{sinc}(s) = \sin(s)/s$. Second assume that the l_j are random and have independent increments $\lambda_j := l_j - l_{j-1}$ that obey exponential distributions with mean l_c. Then the autocorrelation function is

$$\mathbb{E}[m(0)m(x)] = \sigma^2 \exp\left(-\frac{|x|}{l_c}\right)$$

so that the power spectral density is

$$d(k) = \sigma^2 \frac{2l_c}{1 + k^2 l_c^2}.$$

Substituting the general form (24) into system (13) then yields that the decay of the mass is exponential, and that, whatever l_c, the contributions of the main peak and of the secondary peak are equal. Accordingly, the localization length is half the standard value of L_{loc} (compare with equation (15)):

$$N(L) = N_0 \exp\left(-\frac{L}{L_{loc,2}}\right) \tag{26a}$$

$$L_{loc,2} = \frac{V_0^4 l_c}{2\sigma^2}\left(= \frac{V_0^2}{2d(V_0)}\right). \tag{26b}$$

Furthermore, the radiation is emitted half in the forward direction and half in the backward direction, with wavenumbers $-V_0/2$ and $+V_0/2$, respectively.

3.3.3. Fast decay of the power spectral density. We consider that the function $d(k)$ decays fast if its decay rate is faster then any power. For instance, let us assume that the power spectral density has a decay of the form $d(k) \simeq \sigma^2 l_c \exp(-|k|^p l_c^p)$ for some $p > 0$ as $|k| l_c \gg 1$. Then, for $\bar{N} \gg 1$:

$$\bar{d}(\bar{N}) = \frac{\sigma^2 l_c \sqrt{\pi}}{4 l_c^{p/2} \bar{N}^{p/2}} \exp\left(-\bar{N}^p l_c^p\right). \tag{27}$$

Substituting into equation (13a) one finds that the mass first decays as

$$N(L) = N_0 \sqrt[2p]{1 + \frac{l_0^p}{l_c^p} \ln\left(1 - \frac{L}{L_{dis,2}}\right)} \tag{28a}$$

$$L_{dis,2} = \frac{2}{\sqrt{\pi} p \sigma^2 l_c} \frac{V_0^6}{N_0^4} \frac{l_0^{p/2}}{l_c^{p/2}} \exp\left(\frac{l_c^p}{l_0^p}\right). \tag{28b}$$

Then, at distance $L_{cros,3} = (1 - \exp(1 - l_c^p / l_0^p)) L_{dis,2}$ the quantity $4V_0/N^2(L)$ becomes larger than l_c so that we get back the regime described in section 3.2 that is characterized by a decay of the mass as $L^{-1/4}$.

3.3.4. Conclusion. If the power spectral density decays at most as k^{-2} one can only observe an exponential decay of the mass. If this decay is faster than k^{-2}, then one first observes a quick decay of the mass to a low value where the exponential becomes exponential again.

4. The large-mass regime $V_0 \ll N_0$

When $V \ll N$ the scattered mass for the white noise model has broadband spectrum:

$$C(\lambda = \sqrt{NV}x, N, V) = \frac{\pi N^4}{4V^6} \exp\left(-\frac{\pi}{2}\frac{N}{V} - 8\pi x^2\right). \tag{29}$$

Substituting into system (7) yields that the mass of the soliton is almost constant while the velocity decays to zero. This decay is governed by the equation:

$$\frac{\mathrm{d}V}{\mathrm{d}L} = -\frac{\pi}{2^{9/2}} \frac{N_0^{11/2}}{V^{13/2}} D(N_0, V) \exp\left(-\frac{\pi}{2}\frac{N_0}{V}\right) \tag{30}$$

where

$$D(N_0, V) = 2^{5/2} \int_0^\infty \mathrm{e}^{-8\pi x^2}\, d\left(\frac{N_0^2}{4V} + 4N_0 x^2\right) \mathrm{d}x. \tag{31}$$

Note that l_0 is much smaller than l_1 in the large-mass regime. The limit behaviour for large L of velocity V depends on the high-frequency behaviour of the power spectral density of the process m. The exact decay rate of the velocity results from the competition between the terms $D(N_0, V)$ and $\exp(-\pi N_0/2V)$ on the right-hand side of equation (30).

4.1. Sub-exponential decay

We consider that the function d is sub-exponential if $\limsup_{k\to\infty} k^{-1} \ln d(k) = 0$. For instance, a power decay belongs to this class. Then $D(N_0, V) \simeq d\left(N_0^2/(4V)\right)$ and the decay of the right-hand side of equation (30) is imposed by the exponential term. Accordingly, the velocity decays as

$$V(L) \simeq \frac{\pi N_0}{2 \ln L} \qquad L \gg 1. \tag{32}$$

4.2. Exponential decay

Let us now assume that $\limsup_{k\to\infty} \frac{1}{k} \ln d(k) = -l_c$. Then

$$D(N_0, V) \sim \exp\left(-\frac{N_0^2 l_c}{4V}\right). \tag{33}$$

The exponential term $\exp(-\pi N_0/2V)$ and $D(N_0, V)$ are of the same order in equation (30) so that the velocity decays as

$$V(L) \simeq \left(\frac{\pi}{2} + \frac{N_0 l_c}{4}\right) \frac{N_0}{\ln L} \qquad L \gg 1. \tag{34}$$

4.3. Super-exponential decay

In the case when the decay rate of $d(k)$ is faster than any exponential: $\limsup_{k\to\infty} k^{-1} \ln d(k) = -\infty$, the term $D(N_0, V)$ imposes the behaviour of the right-hand side of equation (30). Let us assume for instance that the power spectral density of m is

$$d(k) \sim \sigma^2 l_c \exp\left(-|k|^p l_c^p\right) \qquad |k| l_c \gg 1 \tag{35}$$

for some $p > 1$. The velocity then decreases as the pth root of the logarithm of L:

$$V(L) \simeq \frac{N_0^2 l_c}{4(\ln L)^{1/p}} \qquad L \gg 1. \tag{36}$$

4.4. Conclusion

The logarithmic rate (32) actually represents the maximal decay rate of the velocity. Whatever the process m, the term of the right-hand side of (30) has at least an exponential decay of the type $\exp(-\pi N_0/2V)$, which implies $\liminf_{L\to\infty} V(L) \times \ln(L) \geqslant \pi N_0/2$. However, the decay rate may be much slower. If $D(N_0, V)$ is smaller than $\exp(-\pi N_0/2V)$, then the decay rate is imposed by the power spectral density d. If the spectrum decays faster than some exponential, then the regime corresponding to equation (32) will be slower. Conversely, if the spectrum decays slower than any exponential, then one can only observe the regime (32).

5. Numerical simulations

The results in the previous sections are theoretically valid in the limit case $\varepsilon \to 0$, where the amplitude of the potential goes to zero as ε and the size of the slab goes to infinity as ε^{-2}. In this section we aim to show that the asymptotic behaviours of the soliton can be easily observed in numerical simulations in the case where the potential has a small amplitude, so that its effect appears after a long propagation distance. We use a split-step method to simulate the one-dimensional perturbed NLS equation, and more exactly a fourth-order variant [22], so that we obtain a reliable numerical algorithm which provides accurate solutions even for a long computational time domain. In this section we shall consider a coloured noise with top-hat spectrum. It is a Gaussian white noise that has been filtered so as to cancel the frequencies above

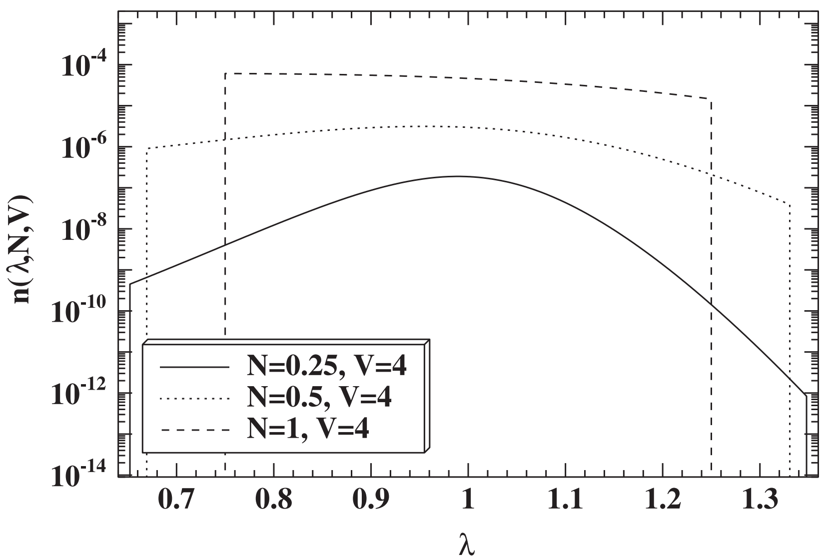

Figure 2. Mass density scattered by a soliton with weak amplitude in the coloured noise model with top-hat spectrum ($d(k) = d(0)\mathbf{1}_{|kl_c|\leqslant 1}$, $d(0) = 1$, and $l_c = 8$). One can see that the main peak around $\lambda = -V/4$ has been cancelled, so that only the secondary peak around $\lambda = V/4$ remains. Moreover, the spectrum becomes more and more concentrated as N decreases.

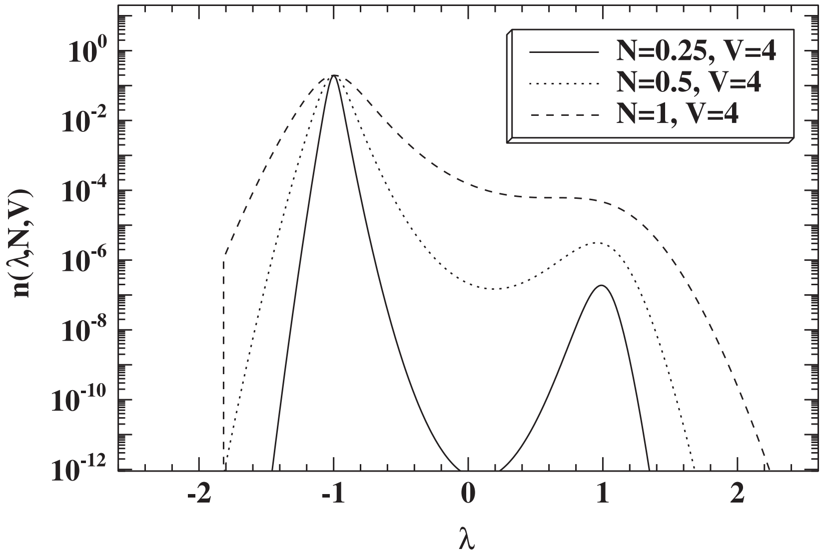

Figure 3. Mass density scattered by a soliton with weak amplitude in the coloured noise model with top-hat spectrum ($d(k) = d(0)\mathbf{1}_{|kl_c|\leqslant 1}$, $d(0) = 1$). Here $l_c = 0.125$ so that this configuration is very close to the white noise model, and the main peak around $\lambda = -V/4$ dominates the spectrum.

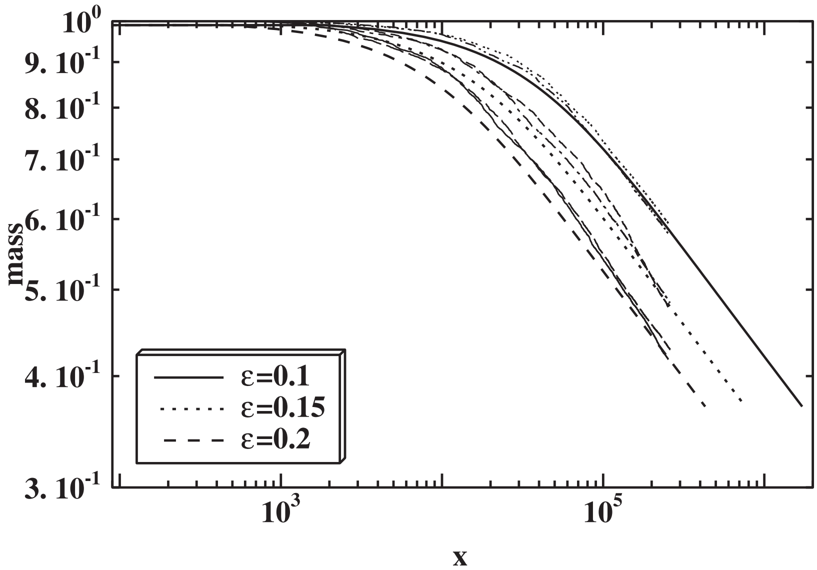

Figure 4. Mass of the soliton as a function of the propagation distance (log–log scales). Here $N_0 = 1$, $V_0 = 4$, the power spectral density is $d(k) = \pi l_c \mathbf{1}_{|kl_c|\leqslant 1}$ where $l_c^{-1} = 0.125$ is the cut-off frequency. We test different values for the small parameter ε. We can clearly see the $x^{-1/4}$ decay after a short transient regime. The thick curves correspond to the theoretical values computed from system (7) (with the scaling $x = L/\varepsilon^2$), while the thin curves correspond to numerical simulations with different realizations of the random potential.

the cut-off frequency $k_c = l_c^{-1}$. As a result the power spectral density is $d(k) = d(0)\mathbf{1}_{|kl_c|\leqslant 1}$ and $d(0) = \pi\sigma^2 l_c$, where $\sigma^2 = \mathbb{E}[m(0)^2]$. In this framework the theoretical scattered mass

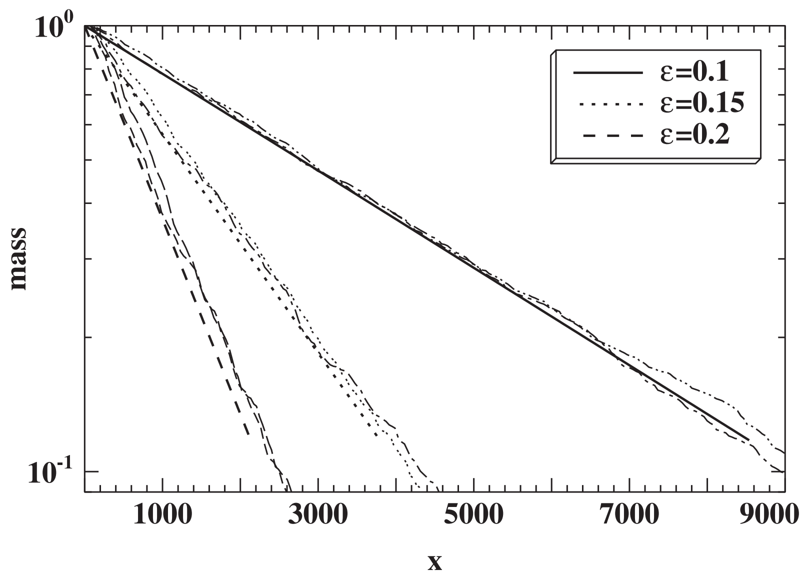

Figure 5. Mass of the soliton as a function of the propagation distance (linear–log scales). Here $N_0 = 1$, $V_0 = 4$, the power spectral density is $d(k) = \pi l_c \mathbf{1}_{|kl_c| \leqslant 1}$ where $l_c^{-1} = 8$ is the cut-off frequency. We test different values for the small parameter ε. We can clearly see the exponential decay. The thick lines correspond to the theoretical values computed from system (7), while the thin lines correspond to numerical simulations with different realizations of the random potential.

density is the scattered mass density of the white noise model restricted to the frequency domain where $\kappa(\lambda, N, V)$ is smaller than l_c^{-1}. Illustrations are given in figures 2 and 3. If l_c is small enough, then we get back the white noise case, while if l_c is large, then the spectrum of the scattered mass is concentrated around the wavenumber $V/2$.

The same dichotomy is found when plotting the evolution of the mass of the soliton: if l_c is small, then the decay is exponential, while if l_c is large, then the decay is power-like (figures 4 and 5). Thus all numerical simulations are in perfect agreement with the theoretical results.

6. Conclusion

We have studied the propagation of a soliton in a nonlinear dispersive medium with a random potential by applying the inverse scattering transform. We have focused on the role of the correlation length of the noise, and especially the importance of long-range correlation. We have demonstrated novel and interesting features in this regime. If the amplitude of the incoming soliton is large, then the mass of the soliton is preserved while the velocity decreases at a slow rate (at most logarithmic) which depends on the high-frequency behaviour of the power spectrum of the random potential. If the amplitude of the incoming soliton is small, then the amplitude of the soliton decays exponentially with the length of the system if the initial velocity of the soliton V_0 is smaller than the width $1/l_c$ of the spectrum of the potential. This regime is similar to that for a white noise potential. If $V_0 l_c > 1$, then a power decay as $L^{-1/4}$ of the amplitude is shown. This regime is original and differs from previously known results. The underlying phenomenon is completely different from the strong localization which is characterized by strong backscattering. The mass of the soliton decays because it emits dispersive radiation in the forward direction.

The importance of the interplay of the correlation length of the perturbation and the characteristic lengths of solitons may be seen as the manifestation of the general phenomenon which has been termed length scale competition [23]. In [24] the effect of a spatially periodic potential on solitons is analysed. This effect is shown to be strongly dependent on the ratio between the wavenumber k_p of the potential and the phase modulation wavenumber $k_0 = V_0/2$ of the soliton. The resonant phenomenon arises when the phase modulation wavenumber and the wavenumber of the potential are matched: $k_0 = k_p$. This is the first example that the characteristic length $1/k_0$ of the soliton, distinct from its width, plays a part in the system behaviour. This competition was exhibited by numerical simulations. As a qualitative explanation [23] the soliton was interpreted as a harmonic oscillator with carrier wavenumber k_0 driven by an external periodic noise $m_p(x) = \cos(k_p x)$:

$$y_{xx} + (k_0^2 + \varepsilon m_p(x))y = 0.$$

It is known that the maximal effect of the noise is obtained when $k_p = k_0 = V_0/2$. On the other hand, it is also known that a harmonic oscillator driven by an external random noise $m(x)$ is unstable and that the Lyapunov exponent that governs the growth of the instability is proportional to the power spectral density of the potential evaluated at $2k_0 = V_0$ [20]. This interpretation is consistent with the main term of equation $(13a)$ which is proportional to $d(V_0)$.

As a global conclusion we can claim that a large-amplitude soliton is more stable than a linear wavepacket with respect to external random perturbations. However, a small-amplitude soliton is less stable than a linear wavepacket with respect to random perturbations, especially those whose correlation lengths are long. When such a configuration arises, the soliton is converted into dispersive radiation that propagates in the forward direction, and whose dynamics is imposed by the standard laws in linear and random media.

This conclusion can be generalized for other systems which are close to the perturbed NLS equation (1), such as a perturbed Ablowitz–Ladik equation [25]. However, the generalization of the procedure as well as the corresponding results is not immediate for all integrable systems. For instance, a perturbed KdV equation requires a specific study where the emission of a soliton gas as well as radiation is proved to be a very general feature [26].

Appendix. Derivation of equation (7)

The proofs of the results stated in section 2 are based on a perturbed inverse scattering transform (IST). The IST consists in a linearization of the homogeneous NLS equation. The main issue is that the solution u may be completely reconstructed at any time from a set of spectral data of an associated eigenvalue problem, the so-called Zakharov–Shabat problem. In this framework the solution u can be described as the superposition of J solitons (corresponding to the discrete eigenvalues λ_j, $j = 1, \ldots, J$) and radiation (characterized by the Jost coefficients associated with the continuous spectrum).

We would also like to remember that there exists an infinite number of quantities which are preserved by the homogeneous NLS equation. They can be represented as functionals of the solution u or in terms of the Jost coefficient a. The first integral of motion is the mass of the wave $N = \int |u|^2 \, \mathrm{d}x$. Denoting $n(\lambda) = -\pi^{-1} \ln |a(\lambda)|^2$, the mass is also given by

$$N = \sum_j 2\mathrm{i}(\lambda_j^* - \lambda_j) + \int n(\lambda) \, \mathrm{d}\lambda. \tag{A1}$$

Of course the Hamiltonian or energy $E = \int |u_x|^2 - |u|^4 \, \mathrm{d}x$ is also preserved. It can be expressed as

$$E = \sum_j \frac{8\mathrm{i}}{3}(\lambda_j^{*3} - \lambda_j{}^3) + 4\int \lambda^2 n(\lambda)\,\mathrm{d}\lambda. \tag{A2}$$

Let us now consider the perturbed NLS equation (1) and list the main steps of the derivation of equation (7) [16].

(a) A priori estimates. The following quantities (mass and energy) are preserved by the perturbed Schrödinger equation (1):

$$N_{tot} = \int |u|^2\,\mathrm{d}x \qquad E_{tot} = \int |u_x|^2 - |u|^4\,\mathrm{d}x + \varepsilon \int H_1(x)\,\mathrm{d}x$$

$$H_1(x) := m(x)|u|^2.$$

Assume that m is a bounded process. Sobolev inequalities then prove that the H^1-norm, the L^4-norm and the L^∞-norm of $u(t,.)$ are uniformly bounded with respect to $t \in \mathbb{R}$ and $\varepsilon \in (0,1)$. Furthermore, $\varepsilon \int H_1(x)\,\mathrm{d}x$ can be bounded uniformly with respect to $t \in \mathbb{R}$ by $N_{tot}\|m\|_\infty \varepsilon$.

(b) Prove the stability of the zero of the Jost coefficient a. The zero corresponds to the soliton. This part strongly relies on the analytical properties of a in the upper complex half plane. Basically, we apply Rouché's theorem so as to prove that the number of zeros is constant. This method is efficient to prove that the zero is preserved, but it does not bring control on its precise location in the upper half-plane. This step is not sufficient to compute the variations of the soliton parameters.

(c) Compute the radiation. The Jost coefficients a and b satisfy coupled equations [21]:

$$\frac{\partial a(\lambda,t)}{\partial t} = 0 + \varepsilon\,(a(\lambda,t)\bar{\gamma}(\lambda,t) + b(\lambda,t)\gamma(\lambda,t))$$

$$\frac{\partial b(\lambda,t)}{\partial t} = -4\mathrm{i}\lambda^2 b(\lambda,t) - \varepsilon\left(a(\lambda,t)\gamma^*(\lambda,t) + b(\lambda,t)\bar{\gamma}(\lambda,t)\right)$$

where $\gamma(\lambda,t) = -\int \mathrm{d}x\, muf_2^2 + mu^* f_1^2$ and $\bar{\gamma}(\lambda,t) = -\int \mathrm{d}x\, mu^* f_1^* f_2 - muf_1 f_2^*$. The functions f_1 and f_2 are the so-called Jost functions and can be computed from the spectral data. From these equations we can estimate the amount of radiation which is emitted during some time interval in terms of mass and energy thanks to (A1) and (A2). We are then able to deduce the evolution equations of the soliton parameters by using the conservation of the total mass and energy. For times of order O(1), since N_{tot} and E_{tot} are conserved, the variations $\Delta(\cdots)$ of the relevant quantities are linked together by the relations

$$0 = 4\Delta\nu + \int \Delta n(\lambda)\,\mathrm{d}\lambda$$

$$0 = 16\Delta\left(\nu\mu^2 - \nu^3/3\right) + 4\int \lambda^2 \Delta n(\lambda)\,\mathrm{d}\lambda + \varepsilon\Delta\left(\int_{\mathbb{R}} H_1(x)\,\mathrm{d}x\right).$$

$\Delta n(\lambda)$ is of the order of ε^2, but the last term in the expression of the total energy is of the order of ε. Thus our strategy is not efficient for estimating the variations of the soliton parameters for times of order O(1). Let us now consider times of order O(ε^{-2}). $\Delta n(\lambda)$ is now of the order of 1, while the last term in the expression of the total energy is of the order of ε by the *a priori* estimates. Thus we can efficiently compute the long-time behaviour of the soliton parameters in the asymptotic framework $\varepsilon \to 0$, when the last term in the expression of the total energy is uniformly negligible. Applying probabilistic limit theorems (approximation–diffusion) establishes that the soliton parameters converge in probability to non-random functions which satisfy the system (7).

(d) Compute the form of the scattered wave. By applying the inverse scattering transform one finds that the total wave is given by the sum of a soliton and of radiation. The radiation looks like any linear dispersive wave far from the soliton, but it has complex structure in the neighbourhood of the soliton. Roughly speaking, the support of the radiation lies in an interval with length of the order of ε^{-2}. Since the L^2-norm is bounded by the conservation of the total mass, we can expect that the amplitude of the radiation is of the order of ε. It can be rigorously proved that the amplitude of the radiation can be bounded above by $K\varepsilon|\ln\varepsilon|$ [16].

References

[1] Abdullaev F Kh, Bishop A R and Pnevmatikos St (ed) 1991 *Nonlinearity with Disorder* (Berlin: Springer)
[2] Tsironis G P and Economou E N (ed) 1998 Fluctuations, nonlinearity and disorder *Phys.* D **113** 115
[3] Kivshar Yu U, Gredeskul S A, Sánchez A and Vázquez L 1990 *Phys. Rev. Lett.* **64** 1693
Kivshar Yu U, Gredeskul S A, Sánchez A and Vázquez L 1992 *Waves Random Media* **2** 125
[4] Bronski J C 1998 *J. Stat. Phys.* **92** 995
[5] Caputo J G, Newell A C and Shelley M 1990 *Integrable Systems and Applications* ed M Balbane, P Loshak, D W McLaughlin and C Sulem (Berlin: Springer)
[6] Knapp R 1995 *Phys.* D **85** 496
[7] Kenna M J, Stanley R L and Maynard J D 1992 *Phys. Rev. Lett.* **69** 1807
[8] Hopkins V A, Keat J, Meegan G D, Zhang T and Maynard J D 1996 *Phys. Rev. Lett.* **76** 1102
[9] Gredeskul S A, Lifshitz I M and Pastur L 1988 *Introduction to the Theory of Disordered Media* (New York: Wiley)
[10] Abdullaev F Kh 1994 *Theory of Solitons in Inhomogeneous Media* (Chichester: Wiley)
[11] Tappert F and Varma C 1970 *Phys. Rev. Lett.* **25** 1108
[12] Wu J, Wheatley J, Putterman S and Rudnick I 1987 *Phys. Rev. Lett.* **59** 2744
[13] Kivshar Yu S and Malomed B A 1989 *Rev. Mod. Phys.* **61** 763
[14] Newell A C 1985 *Solitons in Mathematics and Physics* (Philadelphia, PA: SIAM)
[15] Gredeskul S A and Kivshar Yu U 1992 *Phys. Rep.* **216** 1
[16] Garnier J 1998 *SIAM J. Appl. Math.* **58** 1969
[17] Manakov S V, Novikov S, Pitaevskii J P and Zakharov V E 1984 *Theory of Solitons* (New York: Consultants Bureau)
[18] Middleton D 1960 *Introduction to Statistical Communication Theory* (New York: McGraw-Hill)
[19] Papanicolaou G and Keller J B 1971 *SIAM J. Appl. Math.* **21** 287
[20] Arnold L, Papanicolaou G and Wihstutz V 1986 *SIAM J. Appl. Math.* **46** 427
[21] Karpman V I 1979 *Phys. Scr.* **20** 462
[22] Yoshida H 1990 *Phys. Lett.* A **150** 262
[23] Sánchez A and Bishop A R 1998 *SIAM Rev.* **40** 579
[24] Scharf R and Bishop A R 1993 *Phys. Rev.* E **47** 1375
[25] Garnier J 2001 *Phys. Rev.* E **63** 026608
[26] Garnier J Long-time dynamics of Korteweg–de Vries solitons driven by random perturbations *J. Stat. Phys.* submitted (available at the URL: http://www.cmap.polytechnique.fr/~garnier)